RADIOECOLOGICAL SOFTWARE PACKAGE

Final Report 2000-2003

RESEARCH COLLABORATION PROGRAM:

'MODELLING ENVIRONMENTAL PROCESSES'

APAT- Italian Environmental Protection Agency, Italy
UNSL - San Luis National University, Argentina

Authors

Hugo Velasco, Nicolás Merkis (IMASL, UNSL - Conicet)

Contributors

IMASL
Instituto de Matemática Aplicada San Luis
UNSL - Conicet
Ejército de los Andes, 950 - 5700 San Luis - Argentina

Hugo Velasco
Nicolás Merkis
Emiliano Carreño
Mario Rodríguez
Jimena Juri Ayub
Juan Pablo Toso

APAT
Italian Environmental Protection Agency
Via di Castel Romano, 100
00128 Roma, Italy

Maria Belli
Umberto Sansone

INDEX

1. Introduction

During the Chernobyl accident, large areas of semi-natural ecosystems were affected by radionuclide deposition. Later investigations have shown that the dose risk to man and the environmental radionuclide circulation persists in the long term. Predictive models are essential to take long-term decisions on the management of contaminated environments and to identify the main processes controlling the dynamics of radionuclides inside the ecosystems. The development of decision support software using these models is of importance for a more effective and friendly application of the models to real situations and for the subsequent analysis of the results.

To this end, the triennial scientific collaboration program: *Modeling Environmental Processes* was performed between the Italian Environmental Protection Agency (APAT) and the San Luis National University, Argentina (UNSL). The main objectives of this collaboration were:

1. To develop a general system, based in a Monte Carlo algorithm with the end to calculate the external photon exposure from α-emitter on the ground for different source distributions.
2. To create an interface to link this system with a Geographic Information System
3. To calibrate and validate the system with experimental values obtained for APAT in Italian ecosystems.

As consequence of this collaboration program, the Radioecological Software Package -***RSP***- has been developed. ***RSP*** is a friendly interactive software compatible with Windows 98 operating system or higher. It simulates the behaviour of radionuclides in semi-natural environments and the consequences on the population in terms of the external exposure. ***RSP*** consists of three modules: the first one, *soil mobility*, simulates the vertical transport of radionuclide in soil using the mathematical model *RABES* (Toso & Velasco, 2001). The second module, *soil-to-plant transfer*, simulates the radionuclide soil-to-plant transfer process using the mean soil concentration in the root zone and values of soil-to-plant transfer factor reported in the literature. Soil properties, vegetation types and environmental conditions are taken into consideration in the simulation process. In the third module, *dose assessment*, the dose-rate factor in air at a height of 1 m above ground can be calculated for sources distributed in a slab of finite thickness and sources which are exponentially distributed with depth. The calculations are performed using DAGES Model (Rodríguez & Velasco, 1998), a Monte Carlo algorithm developed to simulate the photon transport for the soil/air configuration. Figure 1 shows the architecture of *RSP* system.

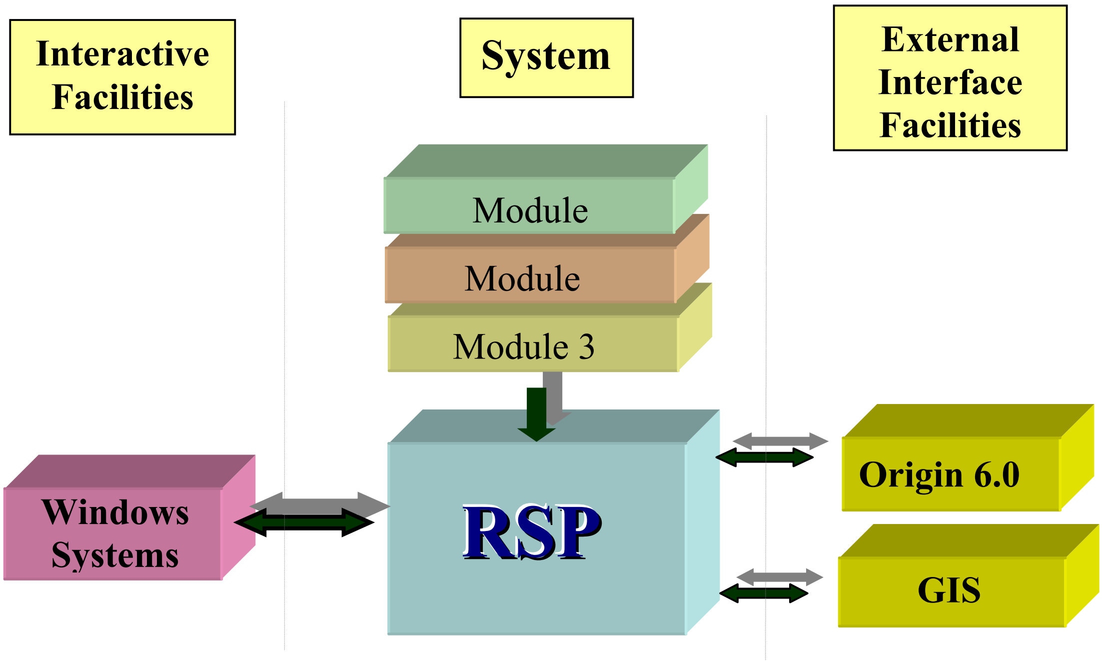

Figure 1. Block structure of the system

RSP was applied to different Italian scenarios. Data used in each case have been provided by the Italian Environmental Protection Agency (APAT).

A web site of the scientific collaboration program (**http://imasl-apat.unsl.edu.ar**) has been developed. From this web site, for which the entry window is shown in figure 2, it is possible to access to the online version of ***RSP*** system.

Figure 2. Index page of the web site: **http://imasl-apat.unsl.edu.ar**.

Annual partial reports of the collaboration and references of publications could be freely obtained from this web site.

2. Literature review

The external exposure from residual photon emitters in soil has been studied extensively in the past. Starting from this external irradiation, the effective dose equivalent has been calculated, usually through the determination of dose-rate conversion factors. The calculations are based on the assumption that the receptor is located a 1 m above the contaminated ground.

Beck and de Planque (1968) and Beck (1972) solve the soil-air photon transport using the polynomial expansion matrix equation to calculate the exposure rate ought to gamma emitters in soil. The dose rate was calculated for a wide range of energy for radionuclides commonly found in the natural environment.

Lowder *et al.* (1964) and Beck *et al.* (1964) introduce the peak area method, a technique for converting measured data from in situ gamma spectrometry into absorbed dose. During the Chernobyl accident, the method was utilised to determine dose rate and activity from deposited fission products (Moberg (1991), Finck (1992)). Today, this method is often incorporated into emergency plans as a rapid procedure for assessing fallout from nuclear accidents.

Kocher and Sjoreen (1985) determine the dose-rate conversion factors. Their calculations are based on the point-kernel integration method and assume that the source concentration at any depth in soil is uniform over an infinite surface parallel to the ground plane. The dose-rate factor is applied to environmental dose assessments by means of the general equation:

$$H(t) = \chi(t) \text{ x } DRF \qquad (1)$$

where H is the external dose rate at time t, χ is the source concentration at the location of the exposed individual, and DRF is the dose-rate factor. DRF depends on the height of the receptor location above ground (this height is usually assumed as 1 m). However for photon emitter in soil, DRF depends on the depth of the source in soil but usually is insensitive to the height of the receptor location above ground for heights of about 10 m or less.

Dose-rate factors in air at a height of 1 m above ground are tabulated for discrete photon energies between 0.01 and 10 MeV and for source depths in soil between 0 and 300 cm. These factors were determined for sources distributed in a slab of finite thickness and sources which are exponentially distributed with depth. For example Velasco *et al*. (1993)

used DRF to evaluate the dose rate in air ought to ^{137}Cs derived of the Chernobyl accident deposited in Italian soils and distributed exponentially with depth.

The methods used to calculate the dose-rate factors involve idealized assumptions concerning vertical and lateral distributions of sources in soil and the extent of shielding provided by the air above ground. Undoubtedly these assumptions are not strictly valid for most realistic exposure situations.

Finck (1994) describes the theory needed to obtain the primary photon fluence for some typical source distribution in the ground. He considers radionuclides deposited on agricultural land which can be mixed into the top layer of the soil by cultivation procedures. This could produce uniform slab sources with thickness depending on the depth of ploughing. Exponentially decreasing source are also contemplated in this analysis.

The geometry used by Finck for calculations of primary photon fluence is based on two semi-infinite volumes of soil and air separated by an infinite plane soil surface (Fig. 3).

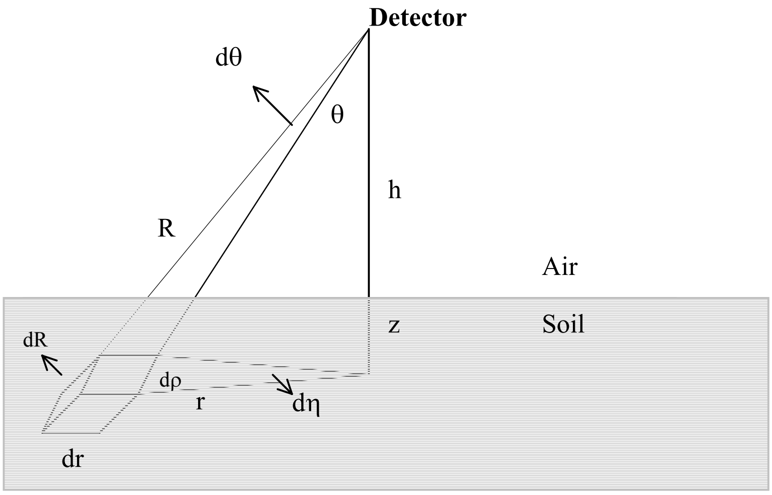

Figure 3. Geometry used in deriving the photon fluence from radionuclides in the ground.

A photon source element is contained in a volume element $\boldsymbol{dV = dr\ dR\ d\rho}$ of soil at depth z below the soil surface. If the photon source is represented by $\boldsymbol{S(z,r,\eta)}$ photons emitted per unit volume of soil as a function of depth z, lateral distance $\boldsymbol{r}$ and azimuthal angle η, then the primary photon fluence at the position of a hypothetical detector at height $\boldsymbol{h}$ above ground and at distance $\boldsymbol{R}$ from this volume element is:

$$d\Phi = \frac{S(z,r,\eta)dV \exp(-\mu_s (R - h \sec\theta) - \mu_a (h\sec\theta)}{4\pi R^2} \tag{2}$$

where θ is the angle between the direction to the volume element and the normal to the air-soil interface, μ_s and μ_a are the mass attenuation coefficients for soil and air respectively. μ_s is usually calculated for soil of composition: 67.5 % SiO_2, 13.5 % Al_2O_3, 10.0 % H_2O, 4.5 % Fe_2O_3 and 4.5 % CO_2 (Beck *et al*. 1972).

The total primary photon fluence can be obtained integrating eqn. (2) over entire photon source in the soil:

$$\Phi = \int_0^{\pi/2} \int_{h\sec\theta}^{\infty} \int_0^{2\pi} \frac{S(z,r,\eta) r \exp(-\mu_s (R - h \sec\theta) - \mu_a (h\sec\theta)}{4\pi R} d\eta \, dR \, d\theta \tag{3}$$

When the source distribution in soil is simple (as uniform or exponentially decrease with depth), the solution of the integral (3) can be easily calculated, but for complicated source distribution, this integral cannot be solved analytically.

If we assume a uniform source distribution ***S*** with infinite depth and infinite lateral extend in the ground, the primary photon fluence is

$$\Phi_{uniform} = \frac{S/\rho_s}{2\mu_s} E_2(\mu_a h) \tag{4}$$

where $E_2(\mu_a h)$ is the exponential integral which is defined, in the general case, as:

$$E_n(x) = x^{n-1} \int_x^{\infty} \frac{e^{-t}}{t^n} dt \tag{5}$$

In the particular case of an superficial infinite plane source, the total primary photon fluence at height ***h*** above ground can be written as following:

$$\Phi_{surface} = \frac{S}{2} E_1(\mu_a h) \tag{6}$$

In the last equation E_1 is the exponential integral of first order.

An exponential decreasing function has been often used to describe the vertical distribution of radionuclides in soil (Velasco *et al.* (1993), (1997)). In this case the source concentration as a function of depth in soil in a determined time is given by:

$$S(z) = S(0) \exp(-\alpha z) \tag{7}$$

where ***S(0)*** is the concentration at the ground surface, α (the alpha-factor of the distribution) is the reciprocal of the relaxation length and it depends on the radionuclide, the soil type and time after deposition. Operating adequately it is possible to obtain the following expression for the total primary photon fluence:

$$\Phi_{\exp} = \frac{S(0)/\rho_S}{2\mu_S/\rho_S}\exp\left(\frac{(\alpha/\rho_S)\mu_S h}{\mu_S/\rho_S}\right)\left[F_1\left(\infty, \frac{-\alpha/\rho_S}{\mu_S/\rho_S}\right) - F_1\left(\mu_S h, \frac{-\alpha/\rho_S}{\mu_S/\rho_S}\right)\right] \quad (8)$$

In this equation the depth has been expressed in mass per unit area ($\rho_s z$) and the function $F_n(t,\alpha)$ is defined as:

$$F_n(t,\alpha) = \int_0^t \exp(\alpha y)\, E_n(y)\, dy \quad (9)$$

Simultaneously, other investigators have used Monte Carlo simulations to calculate effective dose equivalent (O'Brien and Sanna (1976), O'Brien (1978), Jacob et al.(1986), Chen (1991)). In these studies the photon transport in the soil/air interface was simulated and the resultant organ doses to an anthropomorphic phantom was determined. The calculations of Jacob et al. (1986) were based on discrete photon source energies ranging from 0.015 to 6 MeV. The results obtained differed significantly from those of Kocher and Sjoreen (1985). These discrepancies are attributed to the assumption of the isotropic beams in Kocher's calculation.

Huddleston *et al.* (1965) have developed a detailed analysis of the ground roughness effects on the energy and angular distribution ought to gamma emitter from fallout. They investigated three type of terrains: 1) a flat dry-lake bed, 2) a ploughed field with a known degree of roughness and 3) a typical wild desert.

A Monte Carlo algorithm was developed by Chen (1991) to perform the photon transport calculation for the soil/air configuration, in which the soil constituents were assumed to be similar to those of the earth's crust. The calculations are based on the ICRP's concept of effective dose equivalent and the conversion factors published by the ICRP (International Commission on Radiation Protection). Using these calculations is more advantageous for two reasons. First, the ICRP's suggested conversion factors are used for the effective dose equivalent. These conversion factors were not available when the calculations of Jacob et al. (1986) and Kocher and Sjoreen (1985) were formulated. Second, a Monte

Carlo algorithm was tailored to calculate the effective dose equivalent for the soil/air configuration without having to include an anthropomorphic phantom.

In the model proposed by Chen (1991), the photon source is assumed to be distributed uniformly in the soil from the ground surface to a contamination depth, beyond which the soil is uncontaminated (to a total depth). For practical purposes, depths of source up to five mean-free-path lengths of the source photon in the soil and depths of air up to 500 m are considered. To calculate the effective dose-equivalent responses, a Monte Carlo algorithm was developed to track the transport of photons in the soil/air medium as illustrated in Figure 4. Source photons were randomly selected from the contaminated soil zone and their subsequent interactions determined by the probability of occurrence via photoelectric, Compton scattering, and pair-production processes.

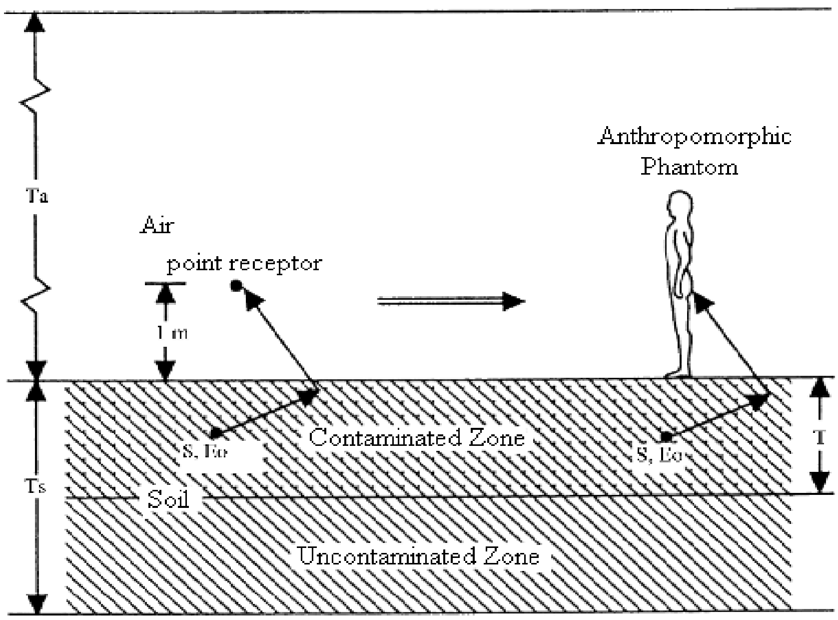

Eo = Photon Energy in MeV in Soil
S = Source Concentration in Soil in Bq cm3
T = Contaminated Soil Thickness (≤5 mfp)
Ta = Air Thickness (500 m)
Ts =Total Soil Thickness (5mfp)

Figure 4. Source/receptor configuration for calculation of dose responses from distributed photon sources in soil.

Clouvas *et al.* (2000) calculate the dose rate conversion factors (absorbed dose rate in air per unit activity per unit of soil mass) 1 m above ground for photon emitters of natural radionuclides uniformly distributed in the soil. In this study are confronted three Monte Carlo codes: the MNCP of Los Alamos (Briesmeister, 1993), the GEANT developed by CERN (GEANT, 1993) and the MC (Clouvas, 1998).

Figure 8 shows the dose rate conversion factor calculated by three Monte Carlo codes for different photon energies. In the same graphic are shown the results obtained from the work of Kocher and Sjoreen (1985) and Chen (1991).

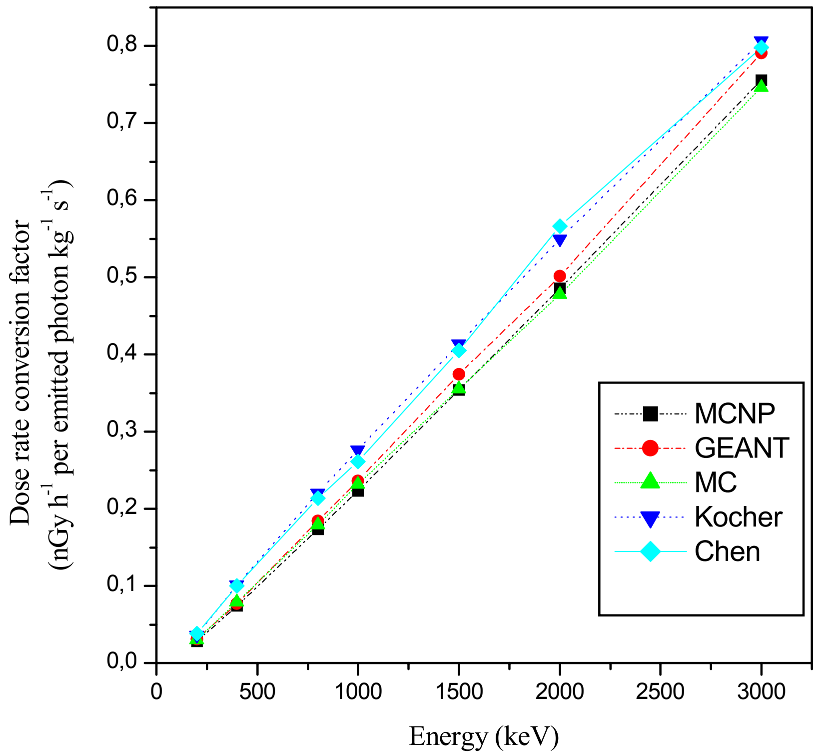

Figure 5. Dose rate conversion factors obtained by the Monte Carlo codes and those deduced from Kocher and Chen as function of the source energy

3. Methods

RABES I model (Velasco et al. 1993, 1997) has been used in the Module 1 of ***RSP*** to determine the temporal variation of the radionuclides vertical profile in soil and its mean concentration in each considered soil layer.

Basically this mathematical model propose that the radionuclide vertical distribution patterns in soil can be described by the following equation:

$$c(z,t) = Q_0 \alpha(t) \exp[-\alpha(t) z] \exp(-\lambda t) \qquad (10)$$

where c *(Bq cm*$^{-3}$*)* is the total radionuclide concentration at depth z *(cm)* and time *t(days after the initial deposition)* , Q_0 *(Bq cm*$^{-2}$ *)* is the initial radionuclide deposition , λ *(d*$^{-1}$*)* is the radioactive decay constant , and α *(cm*$^{-1}$*)* is called the *alpha-factor* .

It is assumed that the *inverse of alpha-factor (* α^{-1} *)* , that we call *L-factor(cm),* has the form

$$L(t) = L_\infty[1 - \exp(k_R t)] \tag{11}$$

where L_∞ *(cm)* is the *L-factor* in the equilibrium, and k_R *(d*$^{-1}$*)* is the rate of change of the vertical profile.

Module 2 of ***RSP*** computes the radionuclide concentration activity in plants using the soil concentration in the root zone (calculated in Module 1) and soil-to-plant transfer factor (TF) reported in the literature. Generic TF values obtained from Frissel et al. (2002) have been incorporated to simulate the radiocaesium transport from soil to plant. The procedure is mainly based on a reference TF value, which depends on soil properties (nutrient status, exchangeable K-content, pH and moisture content). At this stage, vegetation types must also be selected. From this module, the time trend of soil to plant transfer factor and the radionuclide concentration in plants can be obtained.

Running Module 3 of ***RSP*** system, dose-rate factor in air at a height of 1 m above ground can be calculated for sources distributed in a slab o finite thickness and sources which are exponentially distributed with depth. The calculations are performed using DAGES Model, a Monte Carlo algorithm developed to simulate the photon transport for the soil/air configuration.

The steps followed in the simulation process are the following:

a) Photon emission

The photon initial position (source position) is given for his coordinates (z_0, φ_0, θ_0), where z_0 is the soil depth (z = 0 is the soil upper surface), φ_0 and θ_0 are the azimuthal and zenithal angles respectively. The depth z_0 was randomly selected from the contaminated soil zone. φ_0 and θ_0 were randomly selected from the interval [0, 2π] the first and [0, π] the second.

b) Photon track length to the subsequent interaction

The length of the path following by the photon to the next interaction with the medium was determined using the relation (Shultis (1996)):

$$l = -\frac{\ln \delta}{\mu} \qquad (12)$$

where:

l (cm): track length.

δ: random variable in the interval [0,1].

μ (cm^{-1}): energy linear attenuation coefficient.

c) Photon-medium interaction form

The form of the interaction of the photon with the medium is selected having in account the probability of occurrence via photoelectric or Compton scattering. Pair production processes were discarded because of the source energy considered. Angles of scattering by Compton interactions were obtained from the angular distribution described by the Klein-Nishina formula (Evans (1955)).

d) Calculus of the absorbed dose in the receptor

If the photon reaches to the receptor, the absorbed energy by the air mass content in the receptor is calculated according to the procedure proposed by Thomas (1983). The dose absorbed results from the sum of individual contribution of each photon arriving to the receptor, according to the following equation:

$$D = \sum_{i=1}^{N} \Phi(E_i) \cdot \left(\frac{\mu_{ab}(E_i)}{\rho} \right)_{air} \cdot E_i \qquad (13)$$

where

D(Gy): is the absorbed dose in air

$\Phi(E_i)$ (Joule m^{-2}): Photon fluence with energy E_i

$\left(\frac{\mu_{ab}}{\rho} \right)_{air}$ (m^2 gr^{-1}): Energy absorption coefficient in air for energy E_i

Figure 6 shows the results obtained from DAGES Code for the dose rate in air due to a slab of finite thickness in soil with a uniform ^{137}Cs concentration. The values obtained from the analytical procedure proposed by Kocher (1985) and the simulation carried out by Chen (1991) are comparatively shown.

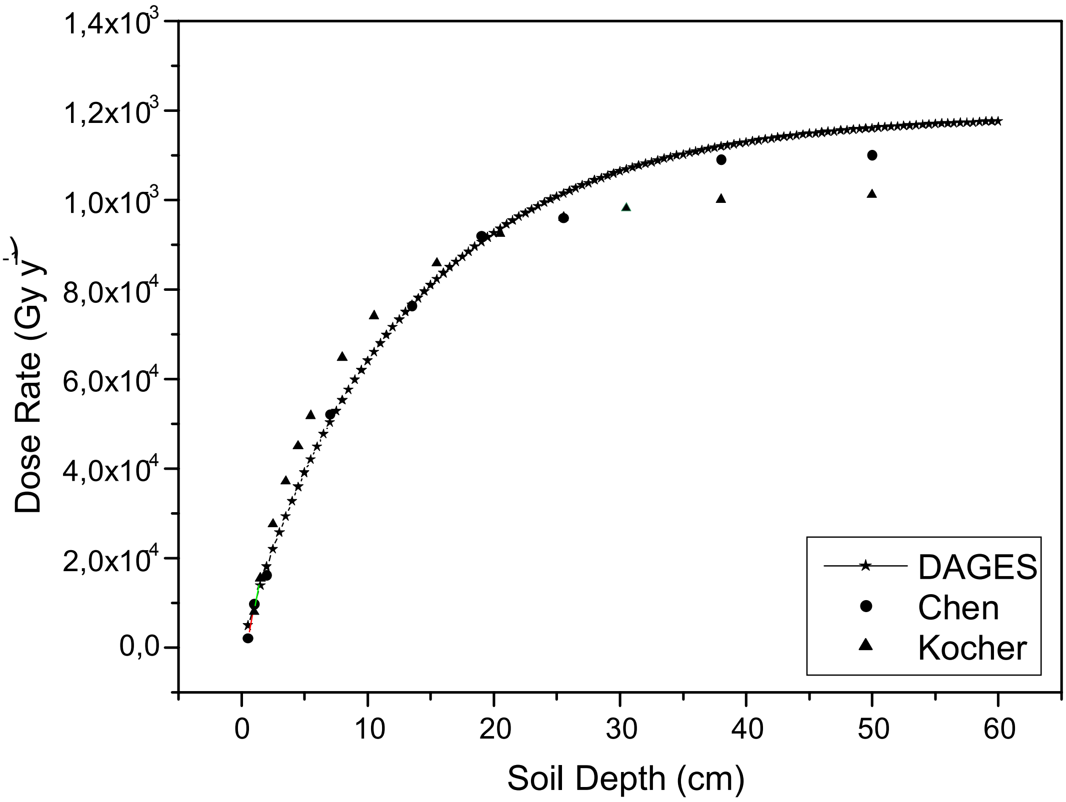

F

igure 6. Dose rate in air due to a uniform distribution of the source (^{137}Cs) into ground

Concentration data used in the validation of ***RSP*** modules 1 and 2 were collected during the period 1989 - 1992, in upland meadows situated in the mountains of the Friuli Venezia Giulia region in the northeast of Italy. Details of experimental procedures and environmental conditions of the studied areas can be obtained in Velasco *et al.*,(1997), (2003).

For the validation of ***RSP*** Module 3, sampling points have been selected in the Calabria and Basilicata Regions (Italy). In an research experimental program carried out by the Italian Environmental Protection Agency, soil samples were performed lengthwise the maritime cost of these regions, determining in each sampling point the soil concentration of ^{40}K and ^{137}Cs together with the external dose rate in air 1 m above soil surface. Experimental procedures carried out in the selected sampling point have been decrypted in ANPA (1997).

4. *RSP* application

4.1 Module 1

Figure 7 shows the windows corresponding to module 1. The values of the parameters and quantities used in the model validation are those shown in the same figure. Validation of this module has been performed using experimental data from Toso & Velasco (2001).

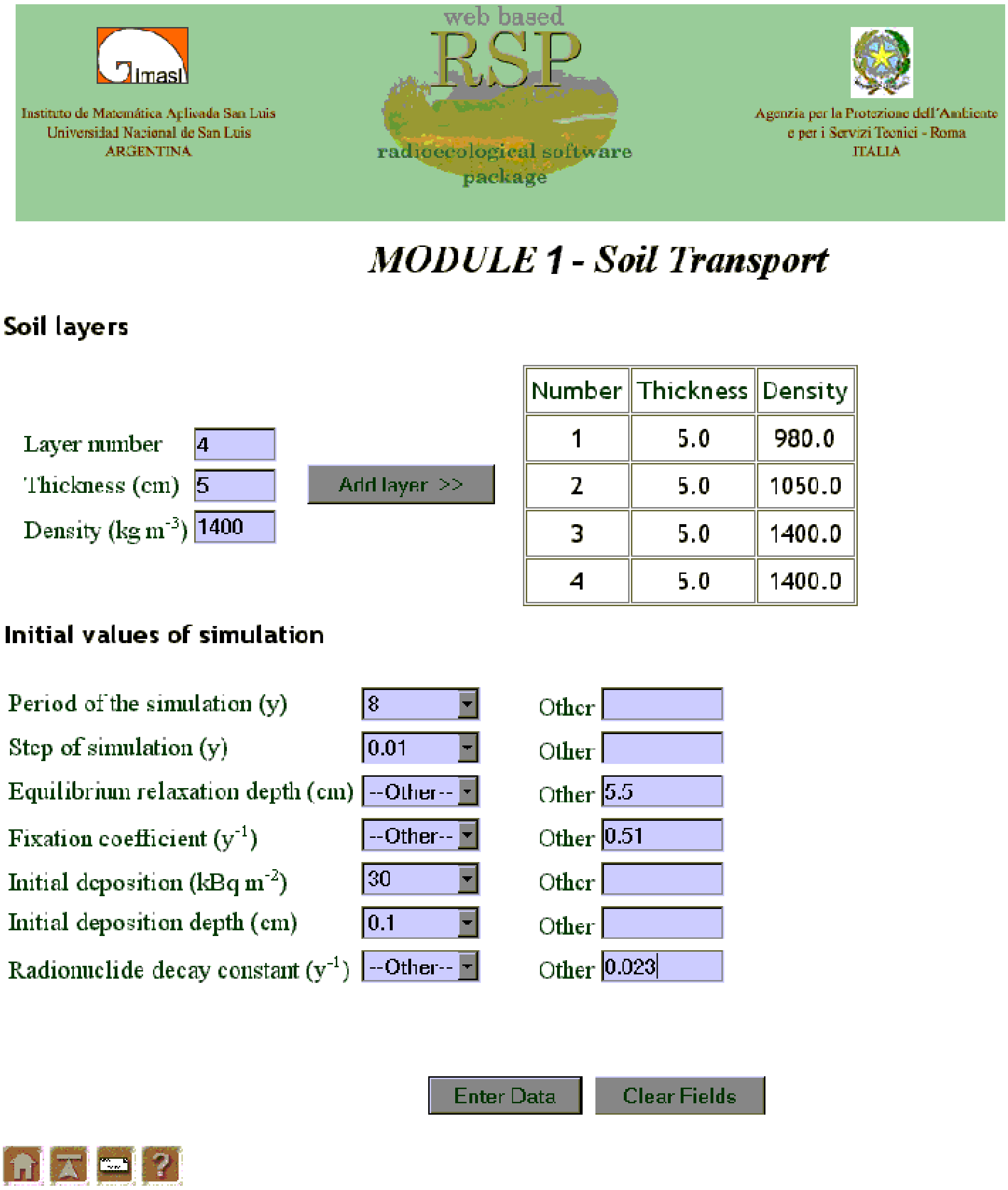

Figure 7. Input window of Module 1 and the parameter values used in the model validation.

Figure 8 represents the relaxation length calculated for the different sampled time and the theoretical curves obtained from the validation of module 1 of ***RSP*** for the input parameters shown in Figure 7.

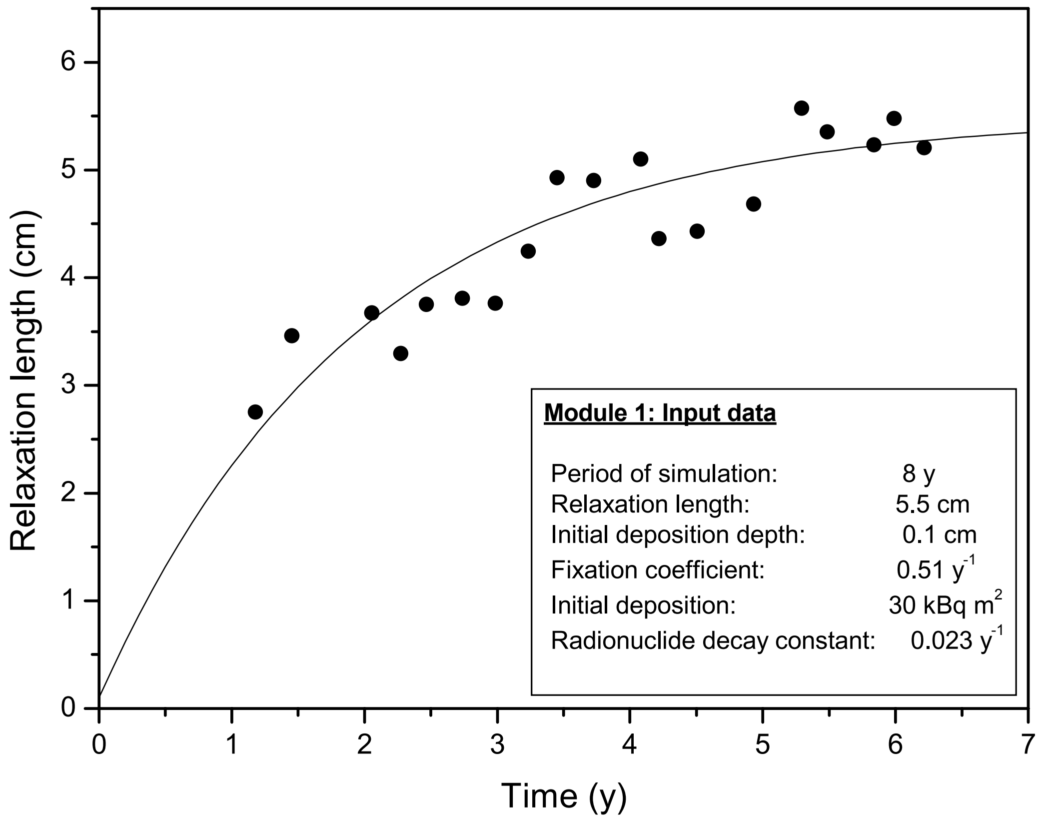

Figure 8. RSP Module 1 validation. Points represent ^{137}Cs relaxation depth measured in a seminatural area (Toso & Velasco (2001)). Curve corresponds to the Module 1 output for the indicated input.

4.2 Module 2

This module permits to determine the radionuclide soil-to-plant transfer using the soil concentration in the root zone (calculated according to Module 1) and values of soil-to-plant transfer factor reported in the literature. Generic TF values obtained from Frissel et al. (1989, 2002) will be incorporated to simulate the radiocaesium transport from soil to plant. The procedure is mainly based on a reference TF value, which depends on soil properties such as nutrient status, exchangeable K-content, pH and moisture content. Different vegetation types can be considered.

Figure 9 shows the module 2 entry windows. The parameter values used in the validation are shown in the same figure. The results obtained from the simulation is shown in Figure 10.

You have provided the following info:

Period of simulation: *5 (y)*	Initial deposition: *27000.0 (Bq m⁻²)*
Initial deposition depth: *0.1 (cm)*	Equilibrium relaxation depth: *4.0 (cm)*
Radionuclide decay constant: *0.023 (y^{-1})*	Fixation coefficient: *0.6 (y^{-1})*
Soil density: *900.0 ($kg\ m^{-3}$)*	Vegetation type: *Grass*
Soil type: *Sand, peats, other*	Nutrient status: *Medium*
J: *0.0030 (y^{-1})* J = Initial soil-to-plant flux density per soil concentration	Release Status: *SSR*

Time unity for tables (y) 1 Other

RUN

Figure 9. Input window of Module 2. Parameter values used in the model validation

Figure 11 shows the experimental values obtained for the radiocaesium plant concentration with the theoretical curve obtained from the module 2 validation. In this figure, dotted lines represent the theoretical range for the plant concentration as function of the elapsed time for deposition.

Results

Time (y)	Soil Concentration ($Bq\ kg^{-1}$)		CR		TFagg ($Bq\ kg^{-2}$)		F ($Bq\ m^{-2}\ y^{-1}$)	Cv ($Bq\ kg^{-1}$)	
	0-10 cm.	0-20 cm.	value	range	value	range		value	range
0.0	3,3E02	1,7E02	2,2E-01	2,0E-02 1,0E00	2,8E-03	2,2E-04 1,1E-02	9,0E01	7,5E01	6,7E00 3,3E02
1.0	3,3E02	1,6E02	1,2E-01	1,1E-02 5,5E-01	1,5E-03	1,2E-04 6,1E-03	4,8E01	4,0E01	3,6E00 1,8E02
2.0	3,2E02	1,6E02	6,8E-02	6,0E-03 3,0E-01	8,4E-04	6,7E-05 3,3E-03	2,6E01	2,1E01	1,9E00 9,5E01
3.0	3,1E02	1,6E02	3,7E-02	3,3E-03 1,7E-01	4,6E-04	3,7E-05 1,8E-03	1,4E01	1,1E01	1,0E00 5,0E01
4.0	3,0E02	1,5E02	2,0E-02	1,8E-03 9,1E-02	2,5E-04	2,0E-05 1,0E-03	7,3E00	6,0E00	5,4E-01 2,7E01
5.0	2,9E02	1,5E02	1,1E-02	1,0E-03 5,0E-02	1,4E-04	1,1E-05 5,5E-04	3,9E00	3,2E00	2,9E-01 1,4E01

TFagg Cv F

Figure 10. Output window of Module 2. Results of the simulation

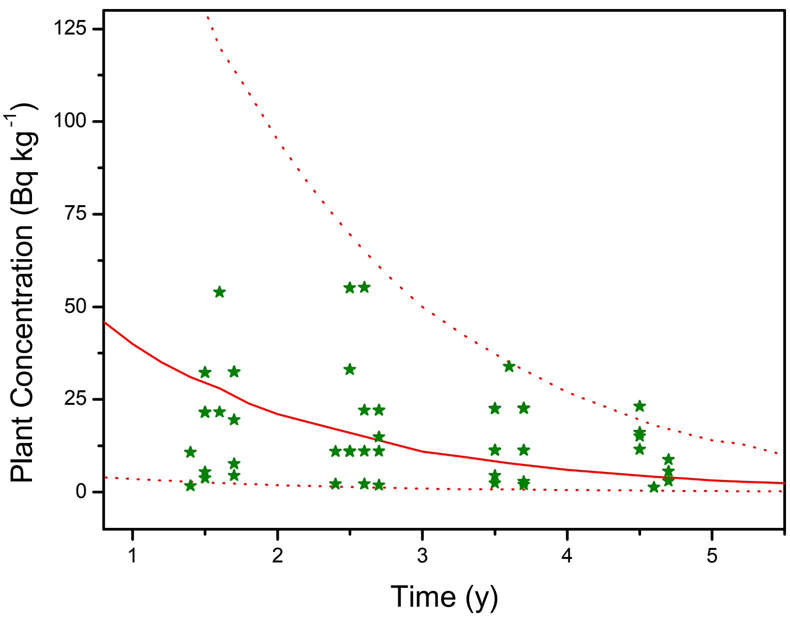

Figure 11. RSP Module 2 validation. Points represent ^{137}Cs plant concentration measured in a seminatural area (Velasco et al (2003)). Curves corresponds to Module 2 output (solid line) and error range (dotted line).

In the column diagram of Figure 12, experimental and theoretical values for the soil to plant activity flux density have been represented.

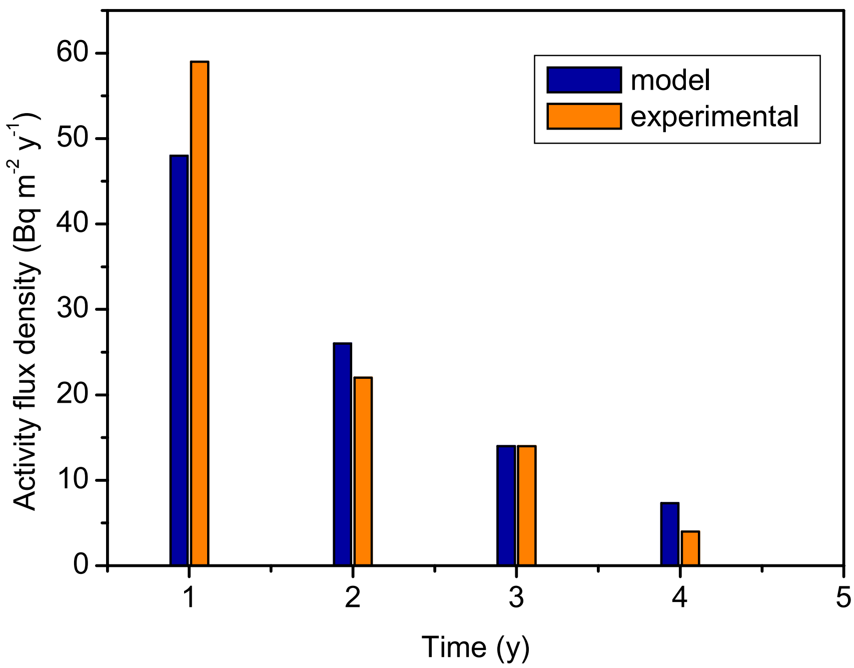

Figure 12. RSP Module 2 validation. Experimental and calculated values for the soil-to-plant activity flux density. Experimental values were obtained from (Velasco et al. (2003)).

4.2 Module 3

Using ***RSP*** Module 3, dose-rate factor in air at a height of 1 m above ground can be calculated for sources distributed in a slab o finite thickness and sources which are exponentially distributed with depth. The calculations are performed using DAGES Model, a Monte Carlo algorithm developed to simulate the photon transport for the soil/air configuration (Rodriguez & Velasco, 1998).

Figure 13 shows the entry windows for module 3. Results of the simulation for these input parameters are shown in Figure 14.

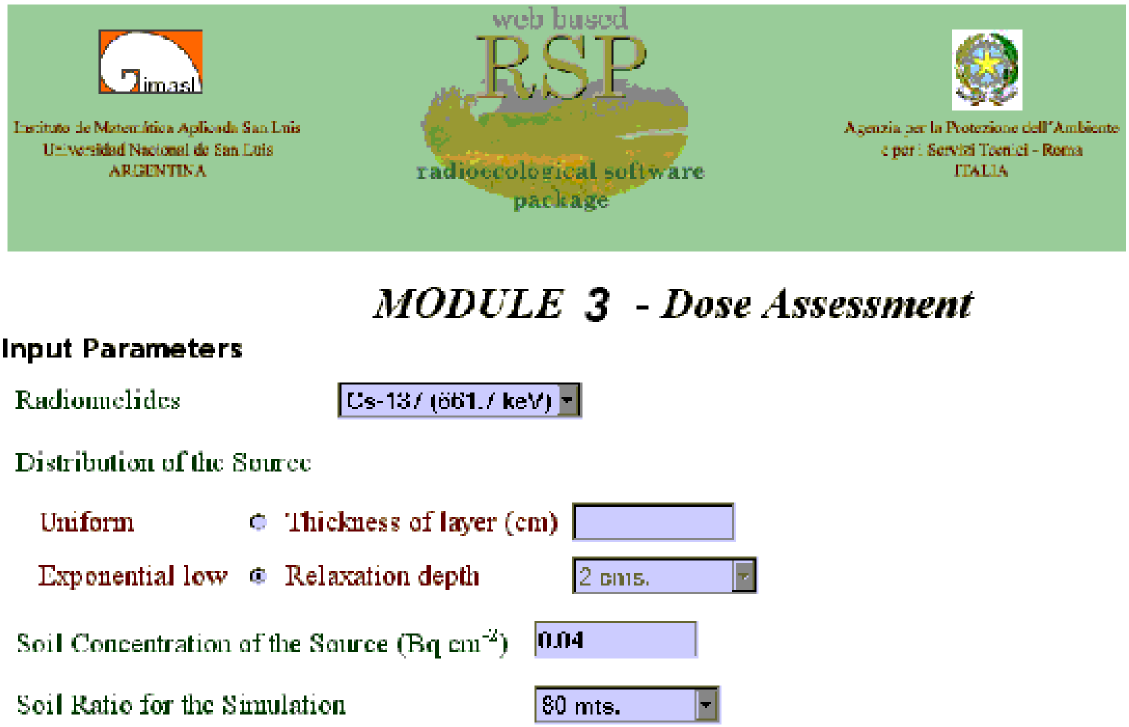

Figure 13. Input window of Module 3.

For the validation of Module 3, two Italian scenarios have been selected in the Calabria and Basilicata Regions. Soil samples were performed lengthwise the maritime cost of these regions, determining in each sampling point the soil concentration of ^{40}K and ^{137}Cs together with the external dose rate in air 1 m above soil surface.

Table 1 summarizes the available information of each sampling point: geographical coordinates, radiocaesium and radiopotassium soil concentration, the measured dose rate and the contributions to external dose rate due to ^{137}Cs soil concentration (using RSP software) and ^{40}K soil concentration (using the methodology proposed in UNCSEAR (2000).

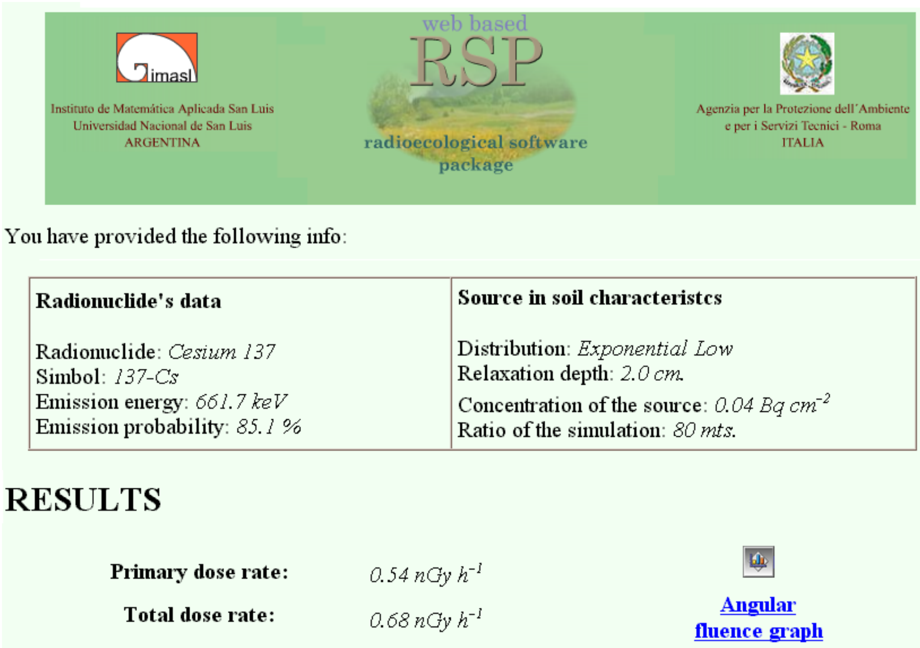

Figure 14. Output window of Module 3. Results of the simulation

Figure 15 shows the ^{137}Cs contribution to the external dose rate. These values have been obtained using ***RSP*** Module 3, considering the sampling points where radiocaesium soil concentration were determined.

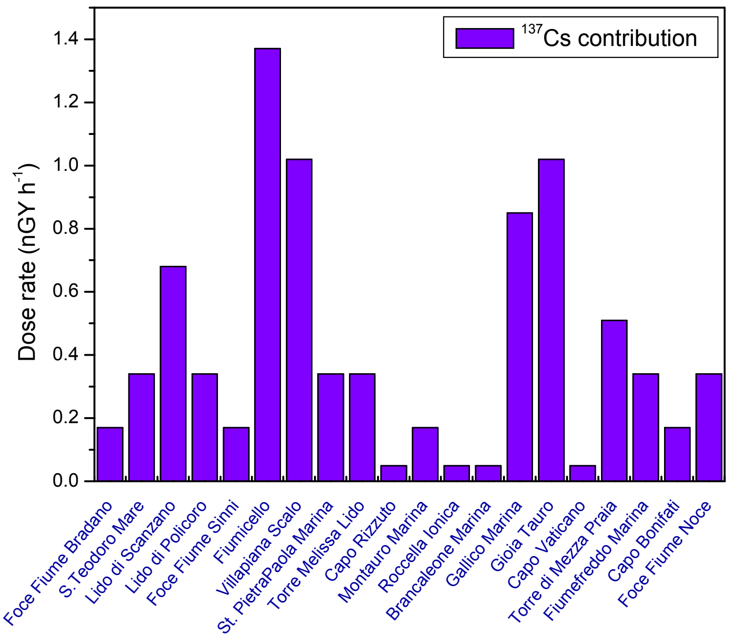

Figure 15. ***RSP*** Module 3 validation. ^{137}Cs contribution to the external dose rate

In Figure 16 has been represented the measured dose rate, in each sampling point, with the sum of the cosmic contribution and the determined dose rate using RSP due to ^{137}Cs and ^{40}K.

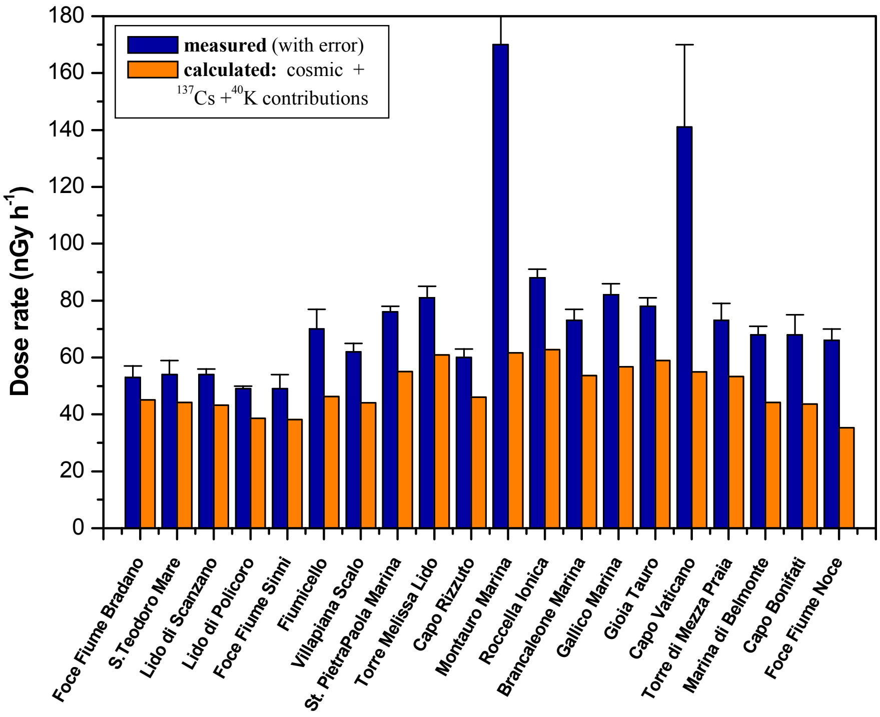

Figure 16. Measured and calculated contribution to the external dose rate in air in different sampling points.

An interface to link *RSP* Module 3 with a Geographic Information System (GIS) has been developed. Using this module it is possible to create an output file with all the necessary information to be used by a GIS.

Figure 17 shows the geographical distribution of the sampled points. MapInfo (1998) has been used as GIS. In this figure the measured dose rate in each sampled points has been represented with differentiated colors according to possible range values.

Figure 18 and 19 show, for ^{137}Cs and ^{40}K respectively, the radionuclide soil concentration and its contribution to the external dose rate. In the case of ^{137}Cs, dose rate has been calculated using *RSP* Module 3, while for ^{40}K, dose rate was determined both according with the UNSCEAR (2000) recommendation and using *RSP* Module 3.

Figure 20 shows a comparison between the 'in situ' measured dose rate and the sum of the cosmic, ^{137}Cs and ^{40}K contributions to the external dose rate. In mean, these three contributions represent nearly the 70% of the measured dose rate.

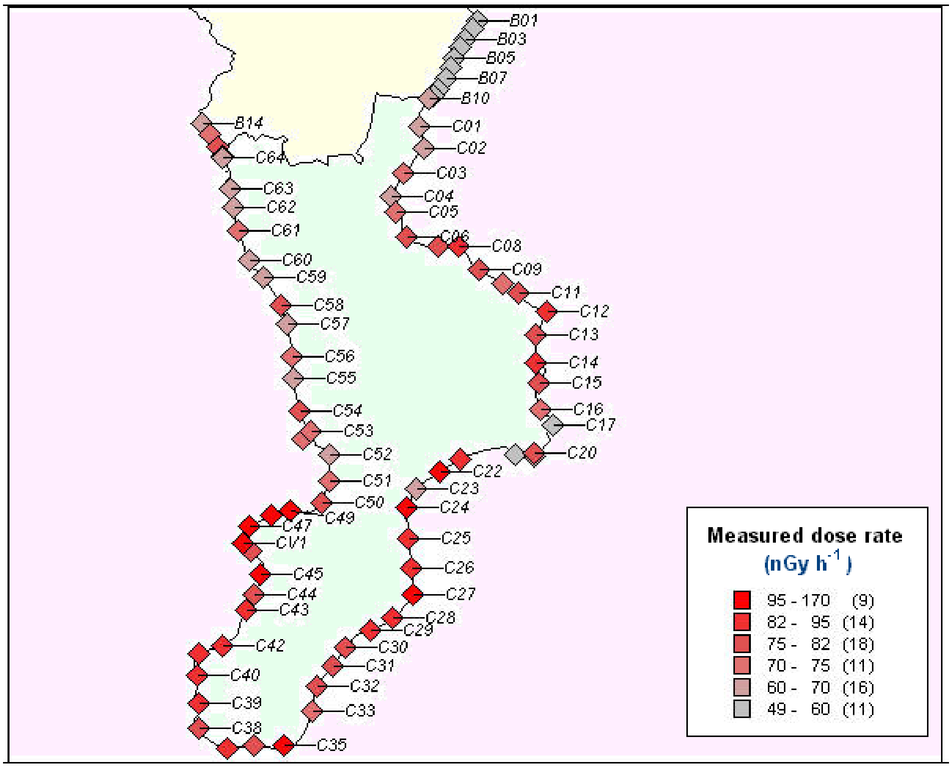

Figure 17. Geographical distribution of the sampling point. Differences in the tonality colors represent the different ranges for the dose rates. Between parenthesis indicates the number of sampling points for each selected range.

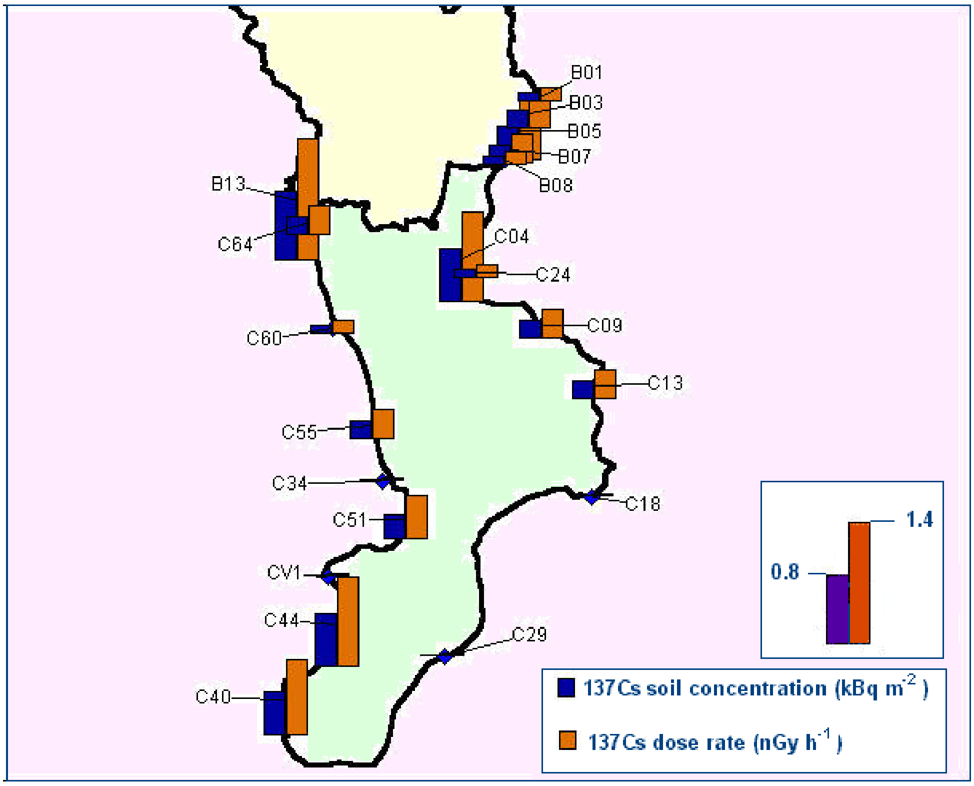

Figure 18. ^{137}Cs soil concentration in each sampling point and its contribution to the external dose rate.

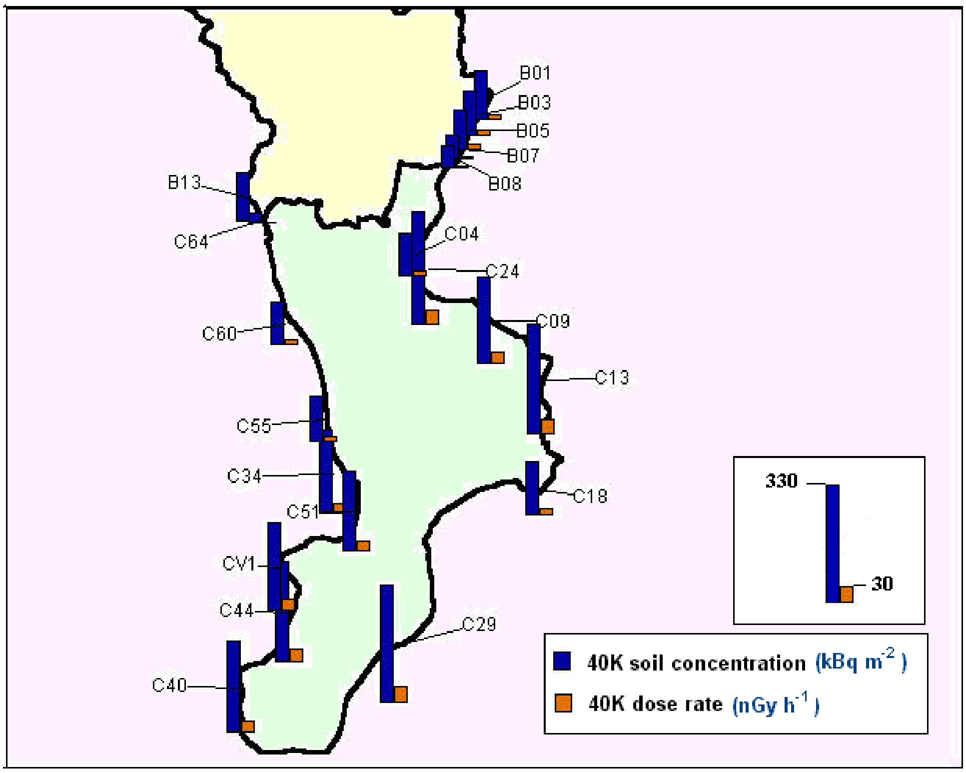

.**Figure 19**. ^{40}K soil concentration in each sampling point and its contribution to the external dose rate.

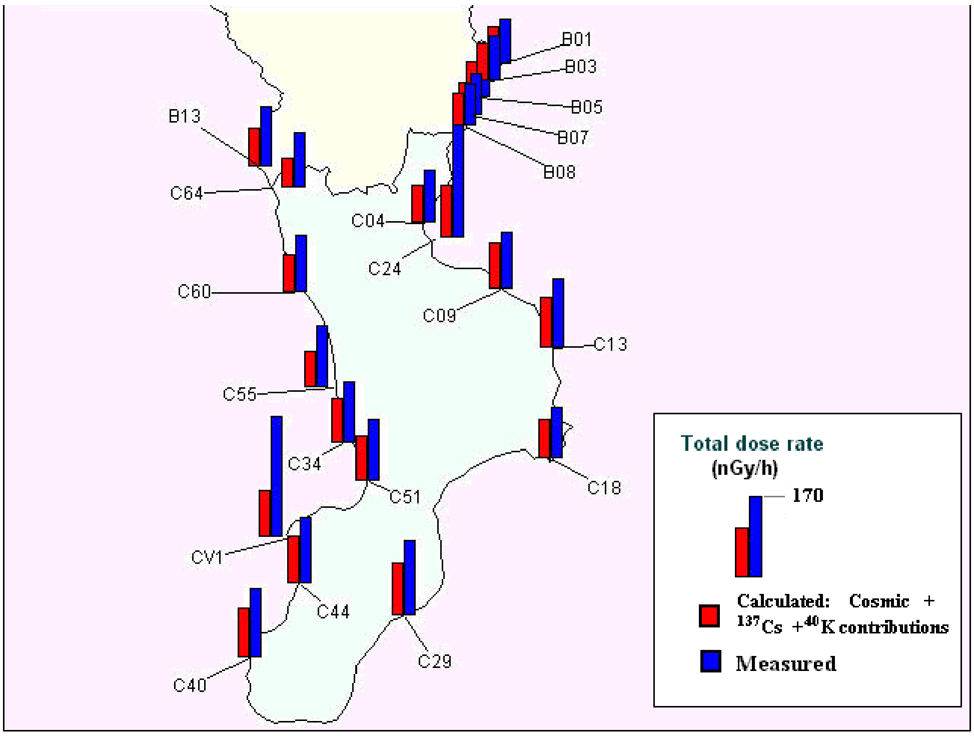

Figure 20. Measured vs. calculated dose rate (sum of the cosmic, ^{137}Cs and ^{40}K contributions) in each sampling point.

Sampled Site	Sampled point	Longitude	Latitude	Soil Concentration (kBq m^{-2})		Measured Dose Rate (nGy h^{-1})	Calculated Dose Rate (nGy h^{-1})		Dose Rate: Cosmic + ^{137}Cs + ^{40}K Contributions (nGy h^{-1})
				^{137}Cs	^{40}K		^{137}Cs Contribution	^{40}K Contribution (UNCSEAR/DAGES)	
Foce fiume Bradano	B01	40° 22.98	16° 51.39	0.1	136	**53 ± 4**	0.17	14.2 / 13.0	**45.1**
Metaponto Lido	B02	40° 21.47	16° 50.10			**53 ± 2**			
S.Teodoro Mare	B03	40° 19.16	16° 48.12	0.2	125	**54 ± 5**	0.34	13.0 / 11.9	**44.2**
S.Basilio Marina di Pisticci	B04	40° 17.60	16° 46.84			**52 ± 5**			
Lido di Scanzano	B05	40° 15.34	16° 45.32	0.4	111	**54 ± 2**	0.68	11.6 / 10.6	**43.3**
Lido di Bufaloria (Scanzano)	B06	40° 13.65	16° 44.61			**53 ± 2**			
Lido di Policoro	B07	40° 11.37	16° 43.17	0.26	66.8	**49 ± 1**	0.36	7.0 / 6.4	**38.7**
Foce del Sinni	B08	40° 09.02	16° 41.43	0.1	63.3	**49 ± 5**	0.17	6.6 / 6.0	**38.2**
Lido di Rotondella	B09	40° 07.97	16° 39.97			**49 ± 5**			
Lido di Nova Siri	B10	40° 07.29	16° 38.94			**60 ± 5**			
Acquafredda	B14	40° 02.15	15° 40.09			**64 ± 4**			
Fiumicello	B13	39° 59.85	15° 41.97	0.8	135.8	**70 ± 7**	1.37	14.2 / 12.9	**46.3**
Marina di Maratea	B12	39° 57.45	15° 44.11			**80 ± 1**			
Maratea Castrocucco	B11	39° 55.56	15° 45.30			**60 ± 2**			
Montegiordano	C01	40° 01.67	16° 36.31			**60 ± 1**			
Stazione di Roseto	C02	39° 57.04	16° 37.75			**64 ± 4**			
Trebisacce	C03	39° 51.97	16° 32.08			**72 ± 3**			
Villapiana Scalo	C04	39° 47.17	16° 29.22	0.6	116	**62 ± 3**	1.02	12.1 / 11.1	**44.1**
Laghi di Sibari	C05	39° 44.11	16° 30.40			**72 ± 2**			
Marina di Schiavonea	C06	39° 39.03	16° 33.15			**80 ± 3**			
Seggio Romano	C07	39° 37.23	16° 41.08			**80 ± 4**			
Mirto Crosia	C08	39° 37.06	16° 46.55			**88 ± 2**			
St. PietraPaola	C09	39° 32.32	16° 51.98	0.2	238	**76 ± 2**	0.34	24.8 / 22.7	**55.0**
Cariati Marina	C10	39° 29.67	16° 57.90			**71 ± 2**			
Crucoli Torretta	C11	39° 27.54	17° 02.21			**80 ± 7**			
Punta Alice	C12	39° 23.81	17° 09.30			**84 ± 2**			
Torre Melissa Lido	C13	39° 18.95	17° 06.72	0.2	299	**81 ± 4**	0.34	31.2 / 28.5	**60.9**
Fasana	C14	39° 13.40	17° 06.71			**92 ± 3**			
Gabella grande	C15	39° 09.17	17° 07.23			**75 ± 3**			
Crotone	C16	39° 03.93	17° 07.91			**72 ± 2**			
Capo Colonna	C17	39° 00.87	17° 10.91			**52 ± 2**			

Capo Rizzuto	C18	38° 54.30	17° 06.10	0.03	147	**60 ± 3**	0.05	15.3 / 13.9	**46.0**
Le Castella	C19	38° 54.58	17° 01.22			**56 ± 5**			
Botricello	C20	38° 55.10	17° 50.97			**80 ± 4**			
S.S. 106 km 201	C21	38° 53.90	16° 47.02			**84 ± 5**			
S.S. 106 km 193	C22	38° 51.28	16° 41.54			**100 ± 4**			
Roccelletto di Borgia	C23	38° 47.82	16° 35.72			**68 ± 4**			
Montauro Marina	C24	38° 43.96	16° 32.97	0.1	309	**170 ± 80**	0.17	32.2 / 29.4	**61.6**
S.S. 106 km 157	C25	38° 37.68	16° 33.60			**84 ± 3**			
Monasterace lido	C27	38° 26.23	16° 34.60			**100 ± 3**			
S.Caterina Ionio Marina	C26	38° 31.66	16° 34.40			**92 ± 7**			
S.S. 106 km 123	C28	38° 21.33	16° 29.46			**88 ± 9**			
Roccella Ionica	C29	38° 19.09	16° 23.82	0.03	323	**88 ± 3**	0.05	33.6 / 30.7	**62.8**
Siderno Marina	C30	38° 15.33	16° 17.08			**81 ± 8**			
Locri Epizep.	C31	38° 11.79	16° 13.72			**80 ± 4**			
Bonamico	C32	38° 07.69	16° 09.67			**80 ± 4**			
Capo Bruzzano	C33	38° 02.62	16° 08.58			**72 ± 1**			
Brancaleone Marina	C34	37° 57.83	16° 06.18	0.03	226	**73 ± 4**	0.05	23.6 / 21.5	**53.6**
Località Doccica	C35	37° 55.38	16° 01.39			**99 ± 6**			
Bova Marina	C36	37° 55.61	15° 53.49			**80 ± 4**			
Melito di porto Salvo	C37	37° 54.97	15° 46.60			**84 ± 7**			
Lazzaro	C38	37° 58.88	15° 39.28			**80 ± 5**			
S.Gregorio	C39	38° 04.07	15° 39.09			**84 ± 1**			
Gioia Tauro	C44	38° 26.22	15° 53.37	0.6	273	**78 ± 3**	1.02	28.4 / 25.9	**59.0**
Palmi Marina	C43	38° 22.91	15° 51.56			**92 ± 7**			
Favazzina	C42	38° 15.63	15° 45.37			**88 ± 2**			
Cannitello Marina	C41	38° 14.14	15° 39.29			**84 ± 4**			
Gallico Marina	C40	38° 09.62	15° 38.96	0.5	251	**82 ± 4**	0.85	26.2 / 23.9	**56.8**
S.Ferdinando Foce F.Mesina	C45	38° 30.29	15° 55.13			**96 ± 6**			
Ioppolo	C46	38° 35.25	15° 52.77			**76 ± 2**			
Scogli di Riace	C47	38° 40.27	15° 52.15			**105 ± 1**			
Marina di Zambrone	C48	38° 42.27	15° 57.86			**100 ± 3**			
Briatico	C49	38° 43.44	16° 02.93			**108 ± 2**			
Pizzo	C50	38° 44.96	16° 11.05			**80 ± 4**			
Torre di Mezza Praia	C51	38° 49.32	16° 13.00	0.3	218	**73 ± 6**	0.51	22.8 / 20.8	**53.3**

Lamezia Terme	C52	38° 54.77	16° 13.19			**68 ± 1**			
Campora S.Giovanni	C54	39° 03.57	16° 05.49			**76 ± 4**			
Torre del Lupo	C53	38° 59.44	16° 08.14			**72 ± 4**			
Marina di Belmonte	C55	39° 10,13	16° 03.79	0.2	125	**68 ± 3**	0.34	13.0 / 11.9	**44.2**
Fiumefreddo Marina	C56	39° 14.62	16° 03.45			**72 ± 5**			
Paola Marina	C57	39° 21.19	16° 02.05			**68 ± 4**			
Fuscaldo Marina	C58	39° 25.05	16° 00.39			**76 ± 3**			
Cetraro Marina	C59	39° 30.85	15° 56.10			**68 ± 3**			
Bonifati	C60	39° 34.32	15° 52.10	0.1	120	**68 ± 7**	0.17	12.5 / 11.4	**43.6**
Diamante	C61	39° 40.43	15° 49.51			**72 ± 4**			
Staz.Crisolia Marina	C62	39° 44.98	15° 48.19			**64 ± 4**			
Staz.Crisolia Marina	C63	39° 48.71	15° 47.22			**64 ± 3**			
Foce F.Noce	C64	39° 55.18	15° 45.51	0.2	31.3	**66 ± 4**	0.34	3.3 / 3.0	**35.3**
Capo Vaticano	CV1	38° 36.79	15° 50.80	0.03	240	**141 ± 29**	0.05	25.0 / 22.8	**54.9**

5. References

Beck H. and dePlanque G. (1968). *The radiation field in air due to distributed gamma-ray sources in ground*. USAEC Report HASL-195.

Beck, H.L., Condon W.M., and Lowder, W. M. (1964). *Spectrometric techniques for measuring environmental gamma radiation*. USAEC Report HASL-150.

Beck, H.L., DeCampo, J. and Gogolak, C. (1972). *In situ Ge(Li) and Na(Tl) gamma-ray spectrometry for the measurement of environmental radiation.* (USAEC Report HASL-258.

Belli M., F.A. Tikhomirov. (1996). *Behaviour of radionuclides in Natural and Semi- Natural Environments.* Final report of ECP-5 Project (1991-1996).

Briesmeister, J. F. (1993). *MCNP-A general Monte Carlo N-particle transport code, version 4[a]*, Los Alamos, NM: Los Alamos National Laboratory; LA-12625.

Bunzl, K., Hillmann, U., Jacob, P., Kretner, R., Schimmack, W., Sanzharova, N., Fesenko, S., Kotik, V., Krouglov, S., Ivanov, Y., Oreshich, L., Levtchuk, S., Arkhipov, A. And Sokolik, G. (1996). *Migration behaviour of radiocaesium in meadow soil and external radiation exposure. In Behaviour of radionuclides in natural and semi-natural environments*. Report of the European Commission EUR 16531 EN. Ed. M. Belli and F. Tikhomirov. pp 94-104.

Clouvas, A., Xanthos, S., Antonopoulus-Domis M., Silva, J. (1998). *Monte Carlo based method for conversion of in situ gamma ray spectra obtained with a portable Ge detector to an incident photon flux energy distribution*. Health Phys. 74:216-230.

Clouvas, A., Xanthos, S., Antonopoulus-Domis M., Silva, J. (2000). *Monte Carlo calculation of dose rate conversion factors for external exposure to photon emitters in soil*. Health Phys. 78(3):295-302.

Chen S. (1991): *Calculation of effective dose-equivalent responses for external exposure from residual photon emitters in soil*. Heath Phys. 60. N3, pp 411-426.

Evans, R.D. (1955). *The atomic nucleus*. New York. McGraw-Hill Book Co.

Fink, R.R. (1992). *Higth resolution field gamma spectrometry and its application to problem in environmental radiology* (Doctoral dissertation, Lund University, Department of Radiation Physics, Malmo).

Fink, R.R. (1994). *The primary photon field from sources in the ground. In Radioecology: Lectures in environmental radioactivity*. Ed. E. Holm. World Scientific. 87-124.

Frissel, M. J., Deb, D. L., Fathony, M. Lin, Y. M., Mollah, A. S., Ngo, N. T., Othman, I., Robison, W. L., Skarlou-Alexiou, V., Topcuoğlu, S., Twining, J. R., Uchida, S. & Wasserman, M. A. (2002). *Generic values for soil-to-plant transfer factor of radiocesium*. Journal of Environmental Radioactivity, 58, 113 - 128.

Frissel, M. J., van Bergeijk K. E. (1989). *Mean transfer values derived by simple statistical analysis.* VIth Report of the Working Group Soil-to-Plant Transfer Factors, IUR, pp. 10-12. RIVM, Bilthoven, The Netherland.

GEANT *Detector description and simulation tool*. Geneva: CERN; Program Library Long Writeup W5013. (1993).

Huddleston, C. M.; Lingler, Q.G.; Burson, Z.G. and Kinkaid, R.M. (1965). *Ground roughness effects on the energy and angular distribution of gamma radiation from fallout*. Health Phys. 11:537-548.

ICRP. *Recomendations of the International Commission of Radiological Protection*. Annals of the ICRP. Vol. 21 N 1-3, (1991).

J. P. Toso and R.H. Velasco.(2001). *Describing the observed vertical transport of radiocesium in specific soils with three time-dependent models*. J. of Environ. Radioactivity 53. (2001) 133-144.

Jacob, P.; Paretzke, H.G.; Rosenbaum, H.; Zankl, M. (1986). *Effective dose equivalent for photon exposure from plane sources on the ground*. Radiat. Prot. Dosim. 14:299-310.

Kocher D. and Sjoreen A. (1985). *Dose-rate convertion factors for external exposure to photon emitters in soil.* Health Phys. V.48 N 2, pp 193-205,

Lowder, W. M., Beck, H.L. and Condon W.M. (1964) *Spectrometric determination of dose rate from natural and fall-out gamma-radiation in the United States*, 1962-63. Nature 4934; pp 745-749.

MapInfo Professional. MapInfo Corporation. Troy. New York. 1998.

Moberg, L. (1991). *The Chernobyl fallout in Sweden*. Swedish Radiation Protection Institute, Stockholm; pp. 9-17.

O'Brien, K. (1978). *Human dose from radiation of terrestrial origin in the nature radiation environment III*. In: Proceeding of the Second International Symposium on the Nature Radiation Environments. Vol. 2. Washington, D.C.: U.S. Department of Energy; Houston, TX. 1163-1250.

O'Brien, K. and Sanna, R. (1976). *The distribution of absorbed dose-rates in humans from exposure to environmental gamma rays*. Health Phys. 30:71-78.

Origin 6.0 . Microcal™ (1999).

Rodríguez M. & Velasco H.: *Determinación de la tasa de dosis debida a gama emisores depositados en el suelo. Simulación de Monte Carlo*. Annals of the Argentinean Physics Association 10, 1998, pp 310-314, (in spanich).

Shultis K. 1996. *Radiation Shielding*. Prince Hall.

Toso, J.P. & Velasco R. H. (2001*). Describing the observed vertical transport of radiocesium in specific soils with three time-dependent model*. Journal of Environmental Radioactivity, 53, 133-144

UNSCEAR, (United Nations Scientific Comitee on the Effects of Atomic Radiation. Report of the General Assembly. 2000

Velasco R H., Toso J., Belli M. and Sansone U. *Radiocesium in Northeastern Part of Italy after the Chernobyl Accident: Vertical Soil Transport and Soil to Plant Transfer*. J. Environ. Radioactivity. Vol 37/1. pp73-84. 1997.

Velasco, H, Juri Ayub, J., Belli, M. and Sansone, U: *Temporal variation of the ^{137}Cs and ^{40}K flux from soil to grass in semi-natural ecosystems.* In press Journal. of Environmental Radioactivity. (2003).

Velasco, R.H., Belli, M., Sansone, U., Menegon, S. *Vertical Transport of Radiocesium in Surface Soils: Model Implementation and Dose-Rate Computation´*. Health Physics, 64, 37-44.(1993).

Velasco, R.H., Belli, M., Sansone, U., Menegon, S. *´Vertical Transport of Radiocesium in Surface Soils: Model Implementation and Dose-Rate Computation*. Health Physics, 64, 37-44.(1993).